



# Quasiclassical study of a termolecular reaction: A more detailed description of the HO<sub>2</sub> collisional stabilization process

César Mogo\*, João Brandão, Wenli Wang, Daniela Coelho, Carolina Rio

Faculdade de Ciências e Tecnologia, Universidade do Algarve, Faro, Portugal

## ARTICLE INFO

### Keywords:

Hydrogen combustion  
Termolecular reactions  
HO<sub>2</sub> collisional stabilization  
Multiple reaction dynamics

## ABSTRACT

We present detailed studies of the collisional stabilization of the HO<sub>2</sub><sup>\*</sup> radical in a mixture of hydrogen atoms and oxygen molecules using molecular dynamic studies and accurate potential energy surfaces. Following previous work on this process's global temperature and pressure dependencies, we analyze each collider's role and estimate specific rate constants and their temperature dependence.

## 1. Introduction

The stabilization reaction:



is known to be of surmounting importance for hydrogen combustion, and research continuously aims at more detailed and precise knowledge of this process. In a recent study, Alexander Konnov presented a new kinetic mechanism for hydrogen combustion, which includes updated kinetics and new transport properties [1]. It agreed with experimental data on the burning velocity measurements for hydrogen flames. It also allowed comprehensible sensitivity and reaction path analyses, although without resolving the problem of the “mixture rules” discussed by Burke and Song [2]. Rafajito et al. presented a kinetic molecular theory-based method identifying reactions of various molecularities in molecular dynamics simulations of bulk gases [3]. They tried to characterize the conditions for which termolecular and higher-order reactions start to impact a complex gas-phase chemistry mechanism. That work also presented two to three-molecule collision frequencies ratio as a function of temperature, density, and collision times. The authors concluded that molecular dynamics results obtained by the group qualitatively agreed with the theoretical predictions. Zhang et al., in a H<sub>2</sub>/O<sub>2</sub> chemical kinetic mechanism for high-pressure combustion, attributed to reaction (1) a rate coefficient uncertainty factor (*UF*) between 1.2 and 2, where:  $k_{\text{stab}}/UF < k_{\text{stab}} < k_{\text{stab}} \times UF$  [4].

The above reference studies demonstrate the scientific interest in the subject and some difficulties encountered. In the present work, we are focused on the HO<sub>2</sub><sup>\*</sup> stabilization process, not considering processes such as the termolecular association reactions, as presented by Burke and Klippenstein [5].

With the aim of better understanding the HO<sub>2</sub><sup>\*</sup> stabilization process, our group recently adapted MReaDy, a Multiprocess Reaction Dynamics program [6–8], to study the evolution of the HO<sub>2</sub> radicals formed by collisions of H atoms with O<sub>2</sub> molecules [9] and following the history of these radicals in the bulk mixture. In addition to the stabilization procedure from Eq. (1), we also took into account the competing dissociation reactions:



In that work, we carried out simulations where H atoms and O<sub>2</sub> molecules were free to react for a set of temperatures (1500, 2000, and 2500 K) and pressures (10, 30, and 50 atm). There, we obtained the formation rates for the stabilized HO<sub>2</sub> complex (as shown in Table 1), as well as for the product channels O<sub>2</sub> and OH. This allowed us to estimate the rate constants  $k_{\text{stab}}$ ,  $k_{\text{O}_2}$  and  $k_{\text{OH}}$ .

As a step further, we applied a Lindemann–Hinshelwood type scheme to reaction (1), decomposing it in several steps:



where, after the formation of a rovibrationally highly excited HO<sub>2</sub><sup>\*</sup> radical in its electronic ground state (Eq. (4)), there are three competing reactions: Eq. (5) - the reverse reaction; Eq. (6) - the chain termination

\* Corresponding author.

E-mail address: [cfmogo@ualg.pt](mailto:cfmogo@ualg.pt) (C. Mogo).

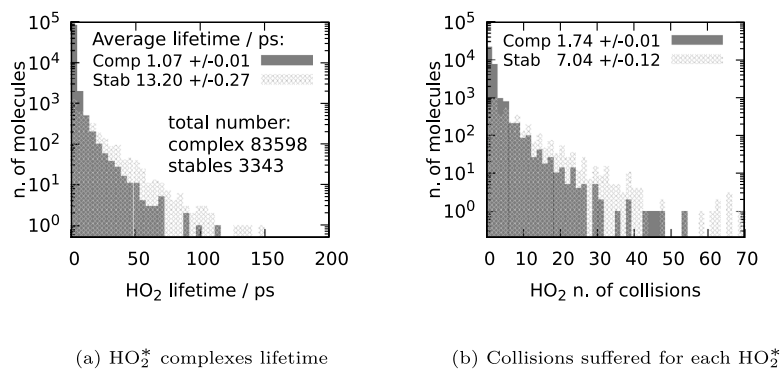


Fig. 1. Fate of the  $\text{HO}_2^*$  radicals in the 2500 K and 50 atm simulation.

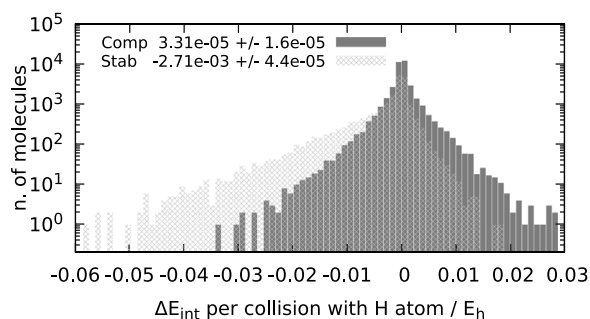


Fig. 2. Histograms for the internal energy exchange per collision of  $\text{HO}_2^*$  complexes with hydrogen atoms denoting different distributions (1500 K and 10 atm).

Table 1

Temperature, pressure and total density settings along with obtained  $\text{HO}_2^*$  formation velocity and  $\text{HO}_2^*$  concentrations as observed in Mogo et al. [9]. Units in K, atm, molec  $\text{cm}^{-3}$  and  $\text{molec}^1 \text{cm}^{-3} \text{s}^{-1}$ .

Temp.	Pres.	[M]	$d[\text{HO}_2]/dt$	$[\text{HO}_2^*]$
1500	10	4.9E+19	$1.09\text{E}+27 \pm 1\text{E}+25$	$1.86\text{E}+17 \pm 7\text{E}+15$
	30	1.5E+20	$2.45\text{E}+28 \pm 1\text{E}+26$	$1.53\text{E}+18 \pm 2\text{E}+16$
	50	2.4E+20	$1.02\text{E}+29 \pm 4\text{E}+26$	$4.11\text{E}+18 \pm 4\text{E}+16$
2000	10	3.7E+19	$3.30\text{E}+26 \pm 2\text{E}+25$	$7.40\text{E}+16 \pm 3\text{E}+15$
	30	1.1E+20	$7.79\text{E}+27 \pm 6\text{E}+25$	$6.94\text{E}+17 \pm 1\text{E}+16$
	50	1.8E+20	$3.27\text{E}+28 \pm 2\text{E}+26$	$1.87\text{E}+18 \pm 3\text{E}+16$
2500	10	2.9E+19	$1.07\text{E}+26 \pm 5\text{E}+24$	$3.87\text{E}+16 \pm 2\text{E}+15$
	30	8.8E+19	$3.22\text{E}+27 \pm 3\text{E}+25$	$3.70\text{E}+17 \pm 9\text{E}+15$
	50	1.5E+20	$1.30\text{E}+28 \pm 1\text{E}+26$	$1.02\text{E}+18 \pm 2\text{E}+16$

process by the stabilization of the  $\text{HO}_2^*$  radical; and Eq. (7) - the chain branching process by the formation of the OH and O radicals. By determining the rate formation of the  $\text{HO}_2^*$  complex and assuming steady state constant value for the complex concentration present in the mixture (right column on Table 1), we were able to determine the rate constants and their Arrhenius parameters, especially for  $k_2$ , the rate of the  $\text{HO}_2^*$  stabilization reaction (Eq. (6)), at different conditions of pressure and temperature.

In that previous work, we focused our attention mainly on the overall kinetic data of these reactions. Here we present a detailed study of the dynamics of the stabilization mechanism and the role of the different collision partners present in the system, namely H atoms,  $\text{O}_2$  molecules, and other  $\text{HO}_2^*$  radicals, taking into account the average energy exchanges in those collisions.

## 2. The adapted MReaDY code

The modifications carried out on the Multiprocess Reaction Dynamics (MReaDY) program [6–8] to study the evolution of the formed  $\text{HO}_2^*$

radicals and follow their history in the bulk mixture is described in detail in our earlier work on this system [9]. In the following, we present a brief description.

MReaDY is a molecular modeling program designed considering the studies of complex chemical processes far from thermal equilibrium. It uses classical dynamics and accurate Potentials Energy Surfaces (PES) to describe the elementary reactions expected to occur in a bulk reactive mixture. This is accomplished using a dynamically defined global potential energy surface and computing all molecular trajectories and collisions simultaneously. According to the interatomic distances, this global PES attributes each atom to a particular molecular system in a defined electronic state, represented by a specific PES, dynamically adjusted during the integration steps. When some interatomic distances fall below a specified threshold, a new molecular species can be formed in a state randomly defined by the electronic states of the colliding partners. The molecular system can also be redefined if any intramolecular distance surpasses a given limit, then the system will dissociate, and a new molecular system will be created. The forces acting on each atom depend on the sum of the PES of its molecular system and the intermolecular forces with the other species present in bulk. Switch functions are used when changing the PES to warrant energy conservation below 2 kcal/mol in the whole simulation process [7]. Although designed to study complex chemical processes far from equilibrium, the MReaDY program can be modified to study multimolecular processes, such as the collisional stabilization of the  $\text{HO}_2$ , which occurs through different collisions with each  $\text{HO}_2$  molecule. This can be accomplished by starting the calculations with the reactants at the desired initial conditions and removing the reaction products once formed. To keep the energy and concentration of the reactants constant, the removed species must be replaced by reactants with the same total energy. Through this process, we replace the usual method of quasiclassical trajectories calculations, consisting of treating each collision independently, by simultaneously calculating a bulk of trajectories able to interact with each other. To focus on the collisional stabilization process, only the collision of an H atom with an  $\text{O}_2$  diatomic can produce a new molecule, and all the remaining collisions proceed through non-reactive PESs that only allow energy transfer between the colliders. In this study, the reactants are the  $\text{H}(^2S)$  atom and the  $\text{O}_2(^3\Sigma_g^-)$  diatomic. By collision, they can form an  $\text{HO}_2^*$  complex. This complex can dissociate back to the reactants, react to products  $\text{OH}(^2\Pi)$  diatomic and O atom ( $^3P$ ), or stabilize to form an  $\text{HO}_2$  radical. These products or the stabilized  $\text{HO}_2$  are removed once formed. We consider that a  $\text{HO}_2^*$  complex has been formed when the energy of this molecular system passes a region where the potential energy is below  $-0.19892 E_h$ , which is 0.2 eV below the  $\text{H} + \text{O}_2$  dissociation energy of  $-0.19157 E_h$ . Then the program starts following the fate of the  $\text{HO}_2^*$  radical, recording its total and internal energy at different steps, namely, at formation, when beginning a collision, at the end of a collision, and finally, when dissociating or stabilizing. We also recorded the involved species, the energy transfer in each collision, and each

**Table 2**

Example of a stabilized HO<sub>2</sub> collision history. We quote the collision partner and its reference, the collision initial and final steps, and the total and internal energy exchanges in  $E_h$ . Each step corresponds to 0.05 fs.

Partner	Reference	ini. step	fin. step	tot. col. steps	tot. ener. ex.	int. ener. ex.
H	049200000000	81 816 396	81 818 686	2290	−0.0014	0.0001
H	008400000000	81 838 708	81 839 130	422	0.0000	−0.0000
H	035300000000	81 859 836	81 860 641	805	−0.0007	−0.0006
H	028000000000	81 866 153	81 868 128	1975	−0.0053	−0.0033
H	007000000000	81 888 544	81 889 490	946	−0.0001	−0.0001
H	020700000000	81 907 876	81 909 399	1523	−0.0023	−0.0038
O <sub>2</sub>	080908100000	81 968 491	81 968 599	108	−0.0000	−0.0000
HO <sub>2</sub>	025108090810	81 969 057	81 969 518	461	0.0000	0.0000
O <sub>2</sub>	080908100000	81 969 519	81 970 430	911	−0.0000	−0.0000
H	042100000000	81 981 805	81 982 870	1065	−0.0003	−0.0025

**Table 3**

Number of collisions and collision lifetime average for collisions between HO<sub>2</sub><sup>\*</sup> that ended up dissociating or stabilized HO<sub>2</sub> complexes with other molecules present in the mixture: H, O<sub>2</sub> and other HO<sub>2</sub><sup>\*</sup> (time units in fs).

T	p	Dissociated HO <sub>2</sub> <sup>*</sup>						Stabilized HO <sub>2</sub>					
		H		O <sub>2</sub>		HO <sub>2</sub> <sup>*</sup>		H		O <sub>2</sub>		HO <sub>2</sub> <sup>*</sup>	
		Coll	$\bar{t}_{coll}$	Coll	$\bar{t}_{coll}$	Coll	$\bar{t}_{coll}$	Coll	$\bar{t}_{coll}$	Coll	$\bar{t}_{coll}$	Coll	$\bar{t}_{coll}$
1500	10	1 959	76.9 ± 1.0	858	275.1 ± 6.7	4	324.5 ± 151.6	888	84.7 ± 3.0	267	336.7 ± 9.2	3	278.3 ± 232.1
	30	15 761	77.3 ± 0.6	7 516	256.7 ± 2.4	199	181.4 ± 11.9	7 358	82.0 ± 1.5	2443	317.2 ± 3.7	89	185.0 ± 18.4
	50	36 799	74.4 ± 0.3	18 230	238.8 ± 1.4	887	171.7 ± 6.0	19 712	79.9 ± 0.6	6951	296.1 ± 2.6	512	201.5 ± 8.4
2000	10	1 054	71.3 ± 1.2	490	218.3 ± 7.0			327	75.4 ± 1.5	112	318.9 ± 12.7		
	30	9 040	68.6 ± 0.8	4 507	219.0 ± 2.5	95	142.5 ± 13.5	3 208	72.9 ± 1.4	1009	291.8 ± 5.8	31	126.0 ± 22.3
	50	24 041	67.5 ± 0.4	12 070	205.9 ± 1.4	361	134.6 ± 6.9	9 329	74.5 ± 1.0	3345	269.4 ± 2.8	158	155.2 ± 10.7
2500	10	681	61.2 ± 1.2	359	185.9 ± 6.8			154	135.5 ± 65.6	53	242.8 ± 13.6		
	30	5 881	62.4 ± 0.8	3 084	193.1 ± 2.6	36	125.3 ± 21.2	1 732	70.0 ± 2.9	609	264.6 ± 5.9	7	87.8 ± 30.3
	50	15 751	60.7 ± 0.3	8 190	183.5 ± 1.5	136	119.3 ± 10.1	4 659	67.6 ± 1.3	1 702	257.1 ± 3.6	39	126.8 ± 17.1

**Table 4**

Average exchange in internal energy per collision for HO<sub>2</sub><sup>\*</sup> complex that dissociated (units in  $E_h$ ). Values for collisions with HO<sub>2</sub><sup>\*</sup> at 1500 K and 10 atm are presented here and on subsequent tables but have no statistical meaning.

T/K	p/atm	Collision partner		
		H	O <sub>2</sub>	HO <sub>2</sub> <sup>*</sup>
1500	10	−0.00009 ± 0.00007	−0.00002 ± 0.00008	−0.00063 ± 0.00057
	30	−0.00002 ± 0.00002	0.00003 ± 0.00003	0.00099 ± 0.00030
	50	0.00003 ± 0.00002	−0.00001 ± 0.00002	0.00065 ± 0.00014
2000	10	−0.00006 ± 0.00013	−0.00001 ± 0.00015	
	30	0.00006 ± 0.00004	−0.00004 ± 0.00005	0.00107 ± 0.00051
	50	0.00009 ± 0.00002	0.00002 ± 0.00003	0.00035 ± 0.00026
2500	10	0.00011 ± 0.00017	0.00007 ± 0.00018	
	30	0.00011 ± 0.00006	−0.00001 ± 0.00007	0.00056 ± 0.00051
	50	0.00005 ± 0.00003	0.00001 ± 0.00004	0.00043 ± 0.00055

event's time step. This HO<sub>2</sub><sup>\*</sup> complex is considered stabilized, forming HO<sub>2</sub> radical, when it is far apart from another system and its total internal energy is below  $-0.19157 E_h$ .

Recent articles have addressed the problem of uncertainty quantification in classical molecular dynamics, pointing out standard procedures and best practices [10,11]. For example, the simulation's running time should be big enough for the system to relax and forget initial conditions, which happens in our case in the first 100 ps, and most important, must be at least a few orders of magnitude greater than the isolated events being studied. In our case, collisions can go up to a few fs, while complexes may live up to 100 ps, whereas the simulations run up to 5 ns.

### 3. Results

Our first conclusion is that stabilizing the HO<sub>2</sub><sup>\*</sup> radical involves many collisions with different partners. As an example, Figs. 1(a) and 1(b) display the histograms for the lifetime and the number of collisions that the dissociated and stabilized HO<sub>2</sub> complexes went through for the 1500 K and 50 atm simulation. Under these conditions, the average lifetime for complexes that did not stabilize is  $1.07 \pm 0.01$  ps, while

for those that stabilized, the average lifetime is  $13.20 \pm 0.27$  ps, showing a difference of one order of magnitude. Regarding the number of collisions, the HO<sub>2</sub><sup>\*</sup> complexes that dissociated suffered on average  $1.74 \pm 0.01$  collisions before dissociation, while stabilized ones collided on average  $7.04 \pm 0.12$  times before being stabilized. So most of the formed complexes will dissociate quickly, but those that stabilize live longer and experience more collisions.

To access the uncertainty of these simulations, one can compare, for example, the average of the total HO<sub>2</sub><sup>\*</sup> complexes lifetime for the one simulation at 2000 K and 30 atm, giving 27 112 complexes, and  $1.131 \pm 0.030$  ps and 27 180 complexes and  $1.191 \pm 0.034$  ps for a second simulation. Hence the averages overlap within the standard uncertainty. By concatenating both simulations, we obtained 54 292 complexes and averaged  $1.161 \pm 0.023$  ps over their lifetime. Such was the procedure for all directly measured variables. Regarding reaction rates and their uncertainties, they were obtained by linear fits to the respective obtained time-dependent data, while for non-observable variables, we used error propagation.

For each HO<sub>2</sub><sup>\*</sup> collision, it was possible to trace its respective total and internal energy exchange. We present in Table 2 the collision history for one HO<sub>2</sub><sup>\*</sup> in a 1500 K and 50 atm simulation that ended

**Table 5**Average exchange in internal energy per collision for HO<sub>2</sub><sup>\*</sup> that stabilized.

T/K	p/atm	Collision partner		
		H	O <sub>2</sub>	HO <sub>2</sub> <sup>*</sup>
1500	10	-0.00311 ± 0.00020	-0.00153 ± 0.00029	0.00070 ± 0.00070
	30	-0.00309 ± 0.00007	-0.00124 ± 0.00008	-0.00298 ± 0.00063
	50	-0.00271 ± 0.00004	-0.00119 ± 0.00005	-0.00192 ± 0.00023
2000	10	-0.00400 ± 0.00041	-0.00183 ± 0.00048	
	30	-0.00345 ± 0.00013	-0.00159 ± 0.00016	-0.00339 ± 0.00117
	50	-0.00307 ± 0.00007	-0.00144 ± 0.00009	-0.00190 ± 0.00050
2500	10	-0.00335 ± 0.00057	-0.00306 ± 0.00066	
	30	-0.00335 ± 0.00017	-0.00198 ± 0.00023	-0.00947 ± 0.00571
	50	-0.00333 ± 0.00011	-0.00167 ± 0.00013	-0.00423 ± 0.00145

**Table 6**Specific rates constants for the HO<sub>2</sub><sup>\*</sup> stabilization.

T/K	p/atm	k <sub>(+H)</sub>	k <sub>(+O<sub>2</sub>)</sub>	k <sub>(+HO<sub>2</sub><sup>*</sup>)</sub>
1500	10	2.09E-10 ± 2.04E-11	3.09E-11 ± 6.34E-12	-2.09E-11 ± 2.10E-11
	30	1.91E-10 ± 6.70E-12	2.56E-11 ± 1.79E-12	1.07E-10 ± 2.29E-11
	50	1.73E-10 ± 4.18E-12	2.66E-11 ± 1.16E-12	9.43E-11 ± 1.15E-11
2000	10	2.10E-10 ± 3.33E-11	3.29E-11 ± 9.54E-12	
	30	1.77E-10 ± 9.59E-12	2.56E-11 ± 2.81E-12	1.33E-10 ± 4.65E-11
	50	1.62E-10 ± 5.83E-12	2.72E-11 ± 1.80E-12	8.34E-11 ± 2.20E-11
2500	10	1.43E-10 ± 3.29E-11	4.51E-11 ± 1.20E-11	
	30	1.62E-10 ± 1.21E-11	3.37E-11 ± 4.38E-12	2.20E-10 ± 1.34E-10
	50	1.46E-10 ± 7.20E-12	2.68E-11 ± 2.34E-12	1.12E-10 ± 3.88E-11

**Table 7**Arrhenius parameters E<sub>a</sub> (J mol<sup>-1</sup>) and A (cm<sup>3</sup> molec<sup>-1</sup> s<sup>-1</sup>) for k<sub>2</sub><sup>Arr</sup>, k<sub>(+H)</sub>, k<sub>(+O<sub>2</sub>)</sub> and k<sub>(+HO<sub>2</sub><sup>\*</sup>)</sub>.

	E <sub>a</sub>	A
k <sub>2</sub> <sup>Arr</sup> [9]	-4.2E3 ± 1.3E3	7.42E-11 ± 6.8E-12
k <sub>(+H)</sub>	-4.8E3 ± 1.7E3	1.22E-10 ± 1.5E-11
k <sub>(+O<sub>2</sub>)</sub>	2.9E3 ± 2.3E3	3.33E-11 ± 5.4E-12
k <sub>(+HO<sub>2</sub><sup>*</sup>)</sub>	6.8E3 ± 6.9E3	1.66E-10 ± 8.5E-11

up stabilizing. Each collision partner is identified by a reference string using four digits to identify each component atom. A hydrogen atom has only four digits, eight for two oxygen atoms of an O<sub>2</sub> molecule, and an HO<sub>2</sub><sup>\*</sup> complex needs twelve, where the first four refer to the hydrogen atom. It demonstrates the interaction of a single HO<sub>2</sub> with all the other kinds of molecules in the mixture.

When comparing the lifetime and the number of collisions, for example, at 1500 K and 10 atm, we obtained 217 stabilized HO<sub>2</sub> complexes with 51 ± 5 ps lifetime having suffered on average 7.9 ± 0.7 collisions. In the case of complexes that took the reverse reaction (Eq. (5)), we found 20 368 complexes with 1.30 ± 0.03 ps lifetime and 0.222 ± 0.005 collision average for each complex, while in the second case, for the O+OH reaction (Eq. (7)), we obtained 215 cases, with 0.67 ± 0.04 ps and 0.14 ± 0.02 collision average. These numbers justify the use of M on the stabilization reaction, which is irrelevant to the reverse and exchange reaction.

Table 3 presents collision averages for each type of collision. The shortest average collision times will correspond to the collisions between HO<sub>2</sub><sup>\*</sup> and H, due to the higher velocities of the latter. The lifetime for a two HO<sub>2</sub><sup>\*</sup> collision is approximately 2/3 faster than for a HO<sub>2</sub><sup>\*</sup> and O<sub>2</sub> collision. As HO<sub>2</sub><sup>\*</sup> and O<sub>2</sub> do not differ much in mass, the main factor contributing to this lifetime difference should be attributed to the higher repulsive potential between the two HO<sub>2</sub><sup>\*</sup> radicals.

As stated before, it was possible to determine the average internal energy exchange for each kind of collision partner. Fig. 2 represents the results obtained for dissociated and stabilized HO<sub>2</sub> complexes and hydrogen collisions at 1500 K and 10 atm.

The values obtained by the three different colliding partners are shown in Tables 4 and 5.

Comparing both tables, the difference between the exchanged energies is up to two orders of magnitude. At first, one could consider that a higher number of degrees of freedom would allow for a better energy transfer. Still, the data points to the opposite direction, with H being on average two times more efficient than O<sub>2</sub>.

#### 4. Specific rate constants

According to Eq. (6), the overall velocity of stabilized HO<sub>2</sub> production can be written as:

$$\frac{d[\text{HO}_2]}{dt} = k_2[\text{HO}_2^*][M]. \quad (8)$$

In our earlier paper [9], we presented the global rate constant dependency on temperature and pressure. In the stabilization process, each HO<sub>2</sub><sup>\*</sup> radical collides with different partners. Despite that, from the results of the present study on the stabilization dynamics of the HO<sub>2</sub><sup>\*</sup> radical, we can estimate the contribution of each collider species and write Eq. (8) as

$$\frac{d[\text{HO}_2]}{dt} = k_{(+H)}[H][\text{HO}_2^*] + k_{(+O_2)}[O_2][\text{HO}_2^*] + k_{(+HO_2^*)}[\text{HO}_2^*]^2. \quad (9)$$

This expression assumes that the contribution of each species is independent of the presence of the others, which should be a valid approximation if we neglect simultaneous collisions of different partners. Although we have found some collisions where a third molecule also interacted, this number is small and can be overlooked in the pressure conditions of our simulations. This is also justified by the small average collision times quoted in Table 3.

For the estimation of each rate constant, k<sub>(+H)</sub>, k<sub>(+O<sub>2</sub>)</sub> and k<sub>(+HO<sub>2</sub><sup>\*</sup>)</sub>, we considered the hypothetical individual stabilization velocities,  $\frac{d[\text{HO}_2]_{(+X)}}{dt}$ . To guess these individual stabilization velocities, we propose to divide the total stabilization velocity proportionally to the fraction of the internal energy exchange due to collisions with each partner:

$$\frac{d[\text{HO}_2]_{(+X)}}{dt} = \frac{\Delta E_{(+X)}^{int}}{\Delta E_{tot}^{int}} \frac{d[\text{HO}_2]}{dt}, \quad (10)$$

where X = H, O<sub>2</sub> and HO<sub>2</sub><sup>\*</sup>. From these individual stabilization velocities, we can estimate specific rate constants by

$$k_{(+X)} = \frac{d[\text{HO}_2]_{(+X)}}{dt} \frac{1}{[X][\text{HO}_2^*]}, \quad (11)$$

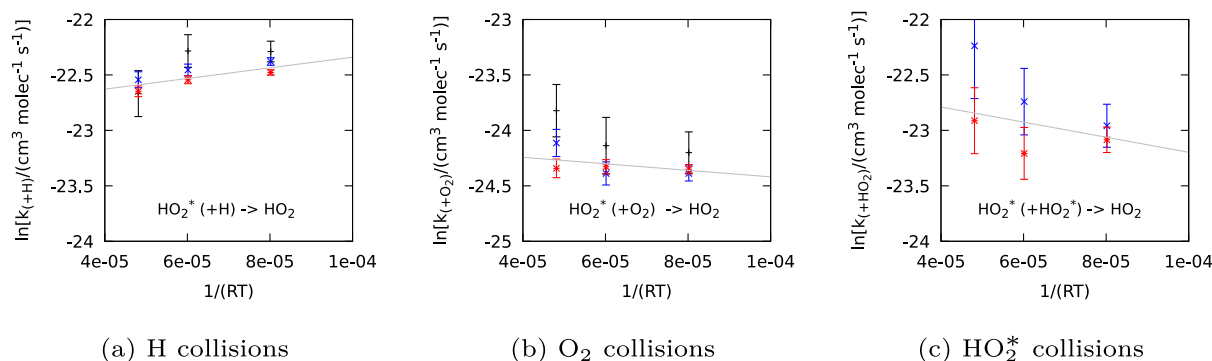


Fig. 3. Stabilization Arrhenius plots for  $k_{(+H)}$ ,  $k_{(+O_2)}$  and  $k_{(+HO_2^*)}$  for 10 atm (+), 30 atm (x) and 50 atm (\*). Errors were weighted for the linear fits, seen in gray.

Table 8

Total and specific rate constants and respective velocities based on the Arrhenius parameters of Table 7 and the concentrations quoted in Table 1. Rate constants and velocities in  $\text{cm}^3 \text{molec}^{-1} \text{s}^{-1}$  and  $\text{molec}^1 \text{cm}^{-3} \text{s}^{-1}$ , respectively.

T/K	p/atm	$k_2^{Arr}$	$V_2$	$k_{(+H)}$	$k_{(+O_2)}$	$k_{(+HO_2^*)}$	$V_{(+H)}$	$V_{(+O_2)}$	$V_{(+HO_2^*)}$	$V_{tot}$	Dev. (%)
1500	10	1.05E-10	9.57E+26	1.81E-10	2.63E-11	9.64E-11	8.22E+26	1.20E+26	3.33E+24	9.45E+26	1.28
	30		2.36E+28				2.03E+28	2.96E+27	2.26E+26	2.35E+28	0.67
	50		1.06E+29				9.08E+28	1.32E+28	1.63E+27	1.06E+29	0.08
2000	10	9.66E-11	2.62E+26	1.64E-10	2.79E-11	1.10E-10	2.23E+26	3.79E+25	6.05E+23	2.61E+26	0.44
	30		7.38E+27				6.26E+27	1.07E+27	5.32E+25	7.38E+27	0.05
	50		3.31E+28				2.81E+28	4.79E+27	3.86E+26	3.33E+28	0.49
2500	10	9.18E-11	1.04E+26	1.55E-10	2.89E-11	1.20E-10	8.79E+25	1.64E+25	1.80E+23	1.05E+26	0.21
	30		2.99E+27				2.52E+27	4.71E+26	1.64E+25	3.01E+27	0.59
	50		1.37E+28				1.16E+28	2.16E+27	1.25E+26	1.39E+28	0.95

Using the different simulations' concentration data quoted in Table 1. The results are presented in Table 6.

Similarly to our previous work [9], we carried out Arrhenius fits of these rate constants ignoring a possible pressure dependence. The results are plotted in Fig. 3 and the Arrhenius parameters so obtained are quoted in Table 7.

To assess the coherence of the estimated specific rate constants obtained with the global rate constant  $k_2^{Arr}$  [9] of our previous work, in Table 8 we compare the rate of the stabilization procedure at the different conditions of temperature and pressure of our simulations using the Arrhenius parameters quoted in Table 7 and the concentration data of quoted in Table 1. Due to the fact that  $[HO_2^*] \ll [H]$ , we consider  $[H] \approx [O_2] \approx [M]/2$ . As expected in the conditions of our simulations, the hydrogen atom emerges as the most effective stabilization agent. The agreement between columns  $V_2$  and  $V_{tot}$  seems very good, as depicted by the deviation quoted in the last columns. This agreement supports the approximation made in this work to compute rate constants for the different colliders. It also shows that using our values for the individual rate constants, we reproduce a global stabilization rate compatible with the experimental data in figure 4 from our previous work on this system [9].

## 5. Conclusion

Complementing our previous work, we gave more details on the  $HO_2^*$  stabilization process in a mixture of hydrogen atoms and oxygen molecules. We showed that, on average, the difference in lifetime between stabilized and dissociated  $HO_2^*$  radicals differs by two orders of magnitude. We noticed that a complex can live on average 20 ps and suffers approximately ten collisions before stabilizing. We have also studied the different partners in the  $HO_2^*$  complex collisions. Furthermore, we present several parameters such as collision time, ranging between 50 fs for H and 200 fs for  $O_2$ , and more interesting, the internal energy exchanges between them, ranging between  $-0.1$  for collisions with other  $HO_2^*$  and  $-0.6 \text{ mE}_h$  for a more efficient H collider. We estimated rate constants for each kind of colliding molecule and their contribution to the overall thermalization process, again with H presenting an efficiency one order of magnitude higher.

## CRediT authorship contribution statement

**César Mogo:** Code development, Data processing, Writing – original draft, Submission. **João Brandão:** General overview, Code development, Writing – original draft. **Wenli Wang:** Original concept, Article corrections. **Daniela Coelho:** Code development. **Carolina Rio:** Concept development, Background research, Writing – original draft.

## Declaration of competing interest

The authors declare that they have no known competing financial interests or personal relationships that could have appeared to influence the work reported in this paper.

## Data availability

Data will be made available on request.

## Acknowledgments

This document results from the research started in the project PTDC/QUI-QUI/100089/2008, funded by the Fundação para a Ciência e a Tecnologia.

## References

- [1] A.A. Konnov, Yet another kinetic mechanism for hydrogen combustion, *Combust. Flame* 203 (2019) 14–22, <http://dx.doi.org/10.1016/j.combustflame.2019.01.032>, URL <https://www.sciencedirect.com/science/article/pii/S0010218019300501>.
- [2] M.P. Burke, R. Song, Evaluating mixture rules for multi-component pressure dependence:  $H_2O_2 (+M) = HO_2 (+M)$ , *Proc. Combust. Inst.* 36 (1) (2017) 245–253, <http://dx.doi.org/10.1016/j.proci.2016.06.068>, URL <http://www.sciencedirect.com/science/article/pii/S1540748916301262>.
- [3] H. Rafatijo, M. Monge-Palacios, D.L. Thompson, Identifying collisions of various molecularities in molecular dynamics simulations, *J. Phys. Chem. A* 123 (6) (2019) 1131–1139, <http://dx.doi.org/10.1021/acs.jpca.8b11686>, pMID: 30657678, arXiv:<https://doi.org/10.1021/acs.jpca.8b11686>.

- [4] Y. Zhang, J. Fu, M. Xie, J. Liu, Improvement of H<sub>2</sub>/O<sub>2</sub> chemical kinetic mechanism for high-pressure combustion, *Int. J. Hydrogen Energy* 46 (7) (2021) 5799–5811, <http://dx.doi.org/10.1016/j.ijhydene.2020.11.083>, URL <https://www.sciencedirect.com/science/article/pii/S0360319920342853>.
- [5] M. Burke, S. Klippenstein, Ephemeral collision complexes mediate chemically termolecular transformations that affect system chemistry, *Nature Chem.* 9 (2017) 1078–1082, <http://dx.doi.org/10.1038/nchem.2842>.
- [6] C. Mogo, J. Brandão, The ready program: Building a global potential energy surface and reactive dynamic simulations for the hydrogen combustion, *J. Comput. Chem.* 35 (17) (2014) 1330–1337, <http://dx.doi.org/10.1002/jcc.23621>.
- [7] C. Mogo, J. Brandão, N-dimensional switch function for energy conservation in multiprocess reaction dynamics, *J. Comput. Chem.* 37 (16) (2016) 1521–1524, <http://dx.doi.org/10.1002/jcc.24361>.
- [8] D.V. Coelho, J. Brandão, C. Mogo, Internal energy and temperature of a carbon nanotube, Fuller. Nanotub. Carbon Nanostruct. (2022) 1–5, <http://dx.doi.org/10.1080/1536383X.2022.2031164>, arXiv:<https://doi.org/10.1080/1536383X.2022.2031164>.
- [9] C. Mogo, J. Brandão, W. Wang, D. Coelho, C. Rio, Quasiclassical study of a termolecular reaction: Application to the HO<sub>2</sub> collisional stabilization process, *Comput. Theor. Chem.* 1209 (2022) 113614, <http://dx.doi.org/10.1016/j.comptc.2022.113614>, URL <https://www.sciencedirect.com/science/article/pii/S2210271X22000275>.
- [10] A. Grossfield, P.N. Patrone, D.R. Roe, A.J. Schultz, D.W. Siderius, D.M. Zuckerman, Best practices for quantification of uncertainty and sampling quality in molecular simulations [article v1. 0], *Living J. Comput. Mol. Sci.* 1 (1) (2018).
- [11] S. Wan, R.C. Sinclair, P.V. Coveney, Uncertainty quantification in classical molecular dynamics, *Phil. Trans. R. Soc. A* 379 (2197) (2021) 20200082.